

# Models of Low Mass Stars in the Local Solar Neighborhood and in Globular Clusters

A Thesis Proposal

Submitted to the Faculty  
in partial fulfillment of the requirements for the  
degree of

Doctor of Philosophy

in

Physics and Astronomy

by

Thomas M. Boudreaux

DARTMOUTH COLLEGE

Hanover, NH

May 10, 2022

The Examining Committee:

---

Dr. Brian Chaboyer

---

Dr. Elisabeth E. Newton

---

Dr. Aaron Dotter

## Abstract

Over its approximately 100 year history stellar modeling has become an essential tool for understanding certain astrophysical phenomena which are not directly observable. Modeling allows for empirical constraints — such as elemental abundances, luminosities, and effective temperatures — to strongly inform non-observables such as **I would say age and mass/radius of single stars** **a core temperature and pressure.** Here we propose a thesis in five parts, related through their use of both modeling and the Dartmouth Stellar Evolution Program (DSEP) to conduct this modeling. In two of the parts of this thesis we will use DSEP, in conjunction with atmospheric boundary conditions generated by collaborators, to build chemically self-consistent models of multiple populations (MPs) in the globular clusters NGC 2808, 47 Tuc, and NGC 6752. We will infer helium abundances across MPs and compare these inferred abundances to those from models which do not consider as careful a handling of a star’s chemistry. The remaining three parts of this thesis will address a recently discovered feature in the Gaia  $G_{BP} - G_{RP}$  color-magnitude-diagram (colloquially the Jao Gap). Throughout this series we will update DSEP’s high-temperature opacity tables to the most modern available (OPLIB from Los Alamos) and show how this change affects the theoretical location of the Jao Gap. Subsequently, we will use synthetic color-magnitude-diagrams (CMDs) — covering the Jao Gap regime — in conjunction with kinematically derived age distributions to test the feasibility of population age-dating by measuring the Jao Gap’s location in a CMD. Finally, we will apply techniques developed in our theoretical testing of Jao Gap based age-dating to the solar neighborhood, attempting to identify coeval groups and roughly age-date them. These five parts will compose the scientific chapters of a thesis to be submitted to the faculty and advising committee no later than the summer term of 2024.

## 1. INTRODUCTION

Throughout last half of the 19th and first decade of the 20th centuries Lane, Ritter, and Emden codified the earliest mathematical model of stellar structure, the polytrope (Equation 1), in *Gaskugeln* (Gas Balls) (Emden 1907).

$$\frac{d}{d\xi} \left( \xi^2 \frac{d\theta}{d\xi} \right) = -\xi^2 \theta^n \quad (1)$$

Where  $\xi$  and  $\theta$  are dimensionless parameterizations of radius and temperature respectively, and  $n$  is known as the polytropic index. Despite this early work, it wasn’t until the late 1930s and early 1940s that the full set of equations needed to describe the structure of a steady state, radially-symmetric, star — the equations of stellar structure — began to take shape as proton-proton chains and the Carbon-Nitrogen-Oxygen cycle were, for the first time, seriously considered as energy generation mechanisms (Cowling 1966). Since then, and especially with the proliferation of computers in astronomy, the equations of stellar structure have proven themselves an incredibly predictive set of models.

There are currently many stellar structure codes (e.g. Dotter et al. 2008; Kovetz et al. 2009; Paxton et al. 2011) which integrate the equations of stellar structure — in addition to equations of state and lattices of nuclear reaction rates — over time to track the evolution of an individual star. The Dartmouth Stellar Evolution Program (DSEP) (Chaboyer et al. 2001; Bjork & Chaboyer 2006; Dotter et al. 2008) is one such, well tested, stellar evolution program.

Here we propose to model low-mass stars in both the solar neighborhood and in globular clusters using DSEP. This work will primarily extend our understanding of stellar physics in two areas: the effects of chemical self-consistency on stellar models (e.g. Dotter et al. 2015) and the time evolution of the core-convective instabilities which ultimately are believed to result in the observed paucity of stars at a Gaia G magnitude of  $\sim 10$  (Jao et al. 2018; Feiden et al. 2021).

### 1.1. Globular Clusters

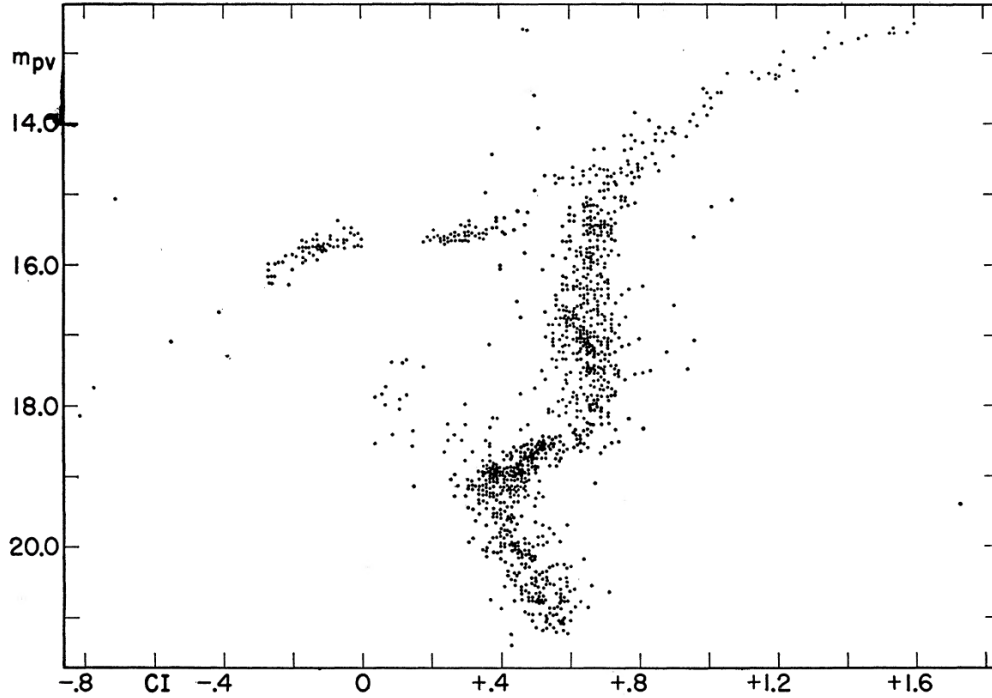


**Figure 1.**  $m_{pg} - m_{pv}$  color-magnitude diagram for the globular cluster M3.

Globular clusters (GC, [Herschel 1814](#)) are among the oldest groupings of stars in the universe, with typical ages greater than 10 Gyr. They are characterized by their compact size — typical half-light radius  $< 10$  pc but up to 10s of pc — and high surface brightness —  $M_V \sim -7$ . For decades, prevailing thought had it that globular clusters were composed of a single stellar population born from a pristine media. Single stellar populations had been assumed, as opposed to multiple stellar population (MPs), due to spectroscopically uniform iron abundances ([Gratton et al. 2012](#)) and very narrow principal sequences (e.g. Figure 1 taken from [Sandage 1953](#); [Stetson & Harris 1988](#)).

These early studies either did not handle — or had very large — photometric uncertainties, masking subtly distinguished features within the CMD. Moreover, given these studies were ground based they were limited to optical bands where colors do not respond strongly to all chemical changes within a star’s atmosphere (water lines, which UV and IR colors will more strongly respond too, are of particular interest).

Despite the canonical view of single populations composing GCs, there has been spectroscopic evidence for chemical inhomogeneities in GCs since the early 1970s (e.g. [Osborn 1971](#)) and by the

late 1980s, as higher resolution photometry became available, multiple clusters were known which exhibited features in their CMDs consistent with either bimodal or multimodal stellar populations (e.g. [Norris 1987](#)).

The first conclusive evidence for MPs came with Hubble Space Telescope (HST) high precision crowded field photometry in which three distinct main sequences in NGC 2808 were identified ([Piotto et al. 2007](#)). Since this discovery, split main sequences have been found in nearly all Milky Way globular clusters studied by HST ([Anderson et al. 2009](#); [Milone et al. 2012](#)). Split stellar populations are believed to be due to enhanced helium abundances, with significant observed star-to-star light-element abundance variation, in their stellar populations formed after the primordial population of stars ([D’Antona et al. 2005](#); [Piotto et al. 2007](#)). When compared to primordial helium mass fractions ( $Y$ ) of  $Y \sim 0.25$  ([Collaboration et al. 2016](#)) or solar helium abundances  $Y \sim 0.27$  ([Vinyoles et al. 2017](#)) these populations have mass fractions as high as  $Y \sim 0.4$ . Helium enhancement is strongly suspected to be the result of an earlier, more massive population dying off, enriching the interstellar medium ([Gratton et al. 2001, 2004, 2012](#)); however, precise formation channels for split stellar populations remain contentious.

Two chapters of this thesis will further constrain the helium enhancement of MPs within globular clusters by modeling their stellar populations in a fully chemically self-consistent manner. Sections [2.4](#) and [2.5](#) address the details of these projects in more detail.

## 1.2. *Local Solar Neighborhood*

[Jao et al. \(2018\)](#) discovered a novel feature in the Gaia  $G_{BP} - G_{RP}$  color-magnitude-diagram. Around  $M_G = 10$  there is an approximately 17% decrease in stellar density of the sample of stars [Jao et al.](#) considered. Subsequently, this has become known as either the Jao Gap, or Gaia M dwarf Gap. Section [2.1](#) will go into more detail regarding the physics underpinning this feature; however, in brief convective instabilities in the core are believed to form for stars straddling the fully convective transition mass (0.3 - 0.35  $M_\odot$ ) ([Baraffe & Chabrier 2018](#)). These instabilities result in stars’ luminosities preferentially evolving either slightly brighter or dimmer than the mass-

luminosity relation around the convective transition mass would naively indicate (Jao & Feiden 2020).

The Jao Gap, inherently a feature of M dwarf populations, provides an enticing and unique view into the interior physics of these stars (Feiden et al. 2021). This is especially important as, unlike more massive stars, M dwarf seismology is currently infeasible due to the short periods and extremely small magnitude’s which both radial and low-order low-degree non-radial seismic waves are predicted to have in such low mass stars (Rodríguez-López 2019). The Jao Gap therefore provides one of the only current methods to probe the interior physics of M dwarfs.

Stellar modeling has been successful in reproducing the Jao Gap (e.g. Feiden et al. 2021; Mansfield & Kroupa 2021) and, with these models, we have begun to understand which parameters constrain the Jao Gap’s location. For example, it is now well documented that metallicity affects the Jao Gap’s color, with higher metallicity stellar populations showing the Jao Gap at consistently higher masses / bluer colors (Mansfield & Kroupa 2021).

Initial testing we have done using DSEP along with articles from both Feiden et al. and Mansfield & Kroupa demonstrates the Jao Gap’s location sensitivity to age, evolving to higher mass regions of the mass-luminosity relation with population age. Per Mansfield & Kroupa (2021) the degree of this location evolution also does not seem to be strongly sensitive to metallicity. Sections 2.2 and 2.3 of this proposal lay out a plan to use this observed age dependence to age-date kinematically separated populations in the solar neighborhood.

## 2. THESIS STRUCTURE

The thesis here proposed will be split into five scientific chapters plus an introduction. Each scientific chapter will consist of work focusing on models of low mass stars.

### 2.1. *Jao Gap & Updated High Temperature Opacities*

A theoretical explanation for the Jao Gap (Figure 2) comes from van Saders & Pinsonneault (2012), who propose that in a star directly above the transition mass, due to asymmetric production and destruction of  $\text{He}^3$  during the proton-proton I chain (ppI), periodic luminosity variations can

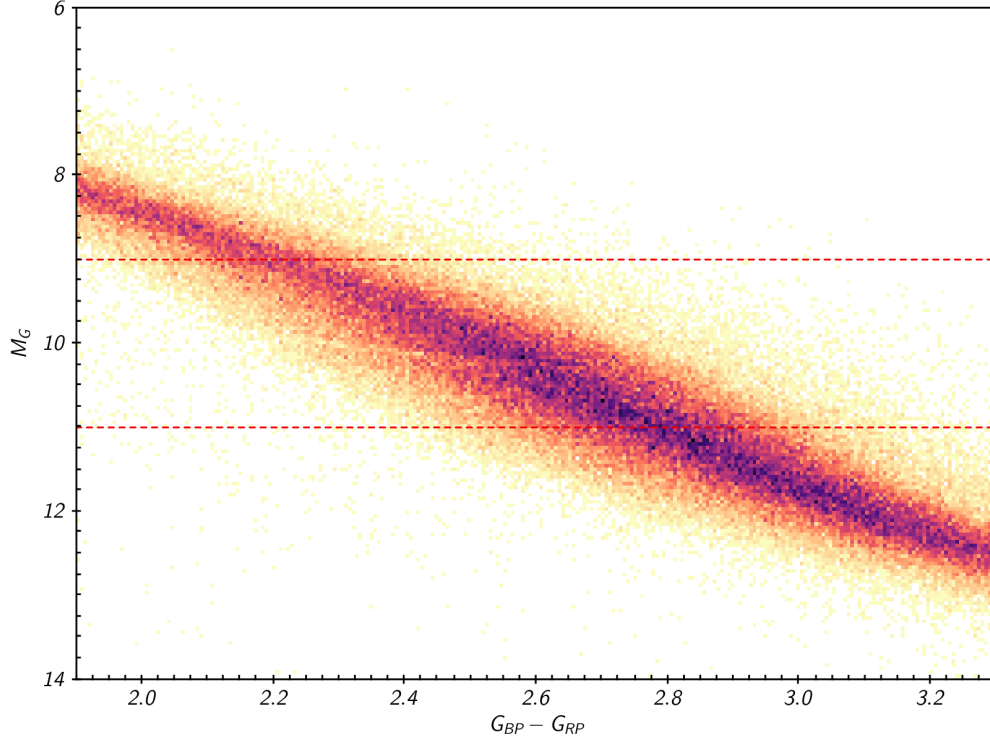


**Figure 2.** Figure 1 from [Jao et al. \(2018\)](#) showing the so called “Jao Gap” at  $M_G \approx 10$

be induced. This process is known as convective-kissing instability. Such a star will descend the pre-MS with a radiative core; however, as the star reaches the zero age main sequence (ZAMS) and as the core temperature exceeds  $7 \times 10^6$  K, enough energy will be produced by the ppI chain that the core becomes convective. At this point the star exists with both a convective core and envelope, in addition to a thin, radiative, layer separating the two. Subsequently, asymmetries in ppI affect the evolution of the star’s convective core.

The proton-proton I chain constitutes three reactions

1.  $p + p \longrightarrow d + e^+ + \nu_e$
2.  $p + d \longrightarrow {}^3\text{He} + \gamma$
3.  ${}^3\text{He} + {}^3\text{He} \longrightarrow {}^4\text{He} + 2p$

Because reaction 3 of ppI consumes  ${}^3\text{He}$  at a slower rate than it is produced by reaction 2,  ${}^3\text{He}$  abundance increases in the core increasing energy generation. The core convective zone will therefore

expand as more of the star becomes unstable to convection. This expansion will continue until the core connects with the convective envelope. At this point convective mixing can transport material throughout the entire radius of the star and the high concentration of  ${}^3\text{He}$  will rapidly diffuse outward, away from the core, again decreasing energy generation as reaction 3 slows down. Ultimately, this leads to the convective region around the core pulling back away from the convective envelope, leaving in place the radiative transition zone, at which point  ${}^3\text{He}$  concentrations build up in the core until it once again expands to meet the envelope. This process repeats until chemical equilibrium is reached throughout the star and the core can sustain high enough nuclear reaction rates to maintain contact with the envelope, resulting in a fully convective star.

### 2.1.1. *Modeling the Gap*

Since the identification of the Gaia M-dwarf gap, stellar modeling has been conducted to better constrain its location, effects, and exact cause. Both [Mansfield & Kroupa \(2021\)](#) and [Feiden et al. \(2021\)](#) identify that the gap’s mass location is correlated with model metallicity — the mass-luminosity discontinuity in lower metallicity models being at a commensurately lower mass. [Feiden et al. \(2021\)](#) suggests this dependence is due to the steep relation of the radiative temperature gradient,  $\nabla_{rad}$ , on temperature and in turn, on stellar mass.

$$\nabla_{rad} \propto \frac{L\kappa}{T^4} \quad (2)$$

As metallicity decreases so does opacity, which, by Equation 2, dramatically lowers the temperature where radiation will dominate energy transport ([Chabrier & Baraffe 1997](#)). Since main sequence stars are virialized the core temperature is proportional to the core density and total mass (Equation 3). Therefore, if the core temperature where convective-kissing instability is expected decreases with metallicity, so too will the mass of stars which experience such instabilities.

$$T_c \propto \rho_c M^2 \quad (3)$$



This strong opacity dependence presents a slight problem where modeling is concerned. With current computational tools it is infeasible to compute opacities on the fly; rather, Rossland Mean opacity ( $\kappa_R$ ) for individual elements must be pre-tabulated over a wide range of temperatures and densities. These opacities can then be somewhat arbitrarily mixed together and interpolated to form opacity lookup-tables. Multiple groups have performed these calculations and subsequently made tables available to the wider community, these include the Opacity Project (OP [Seaton et al. 1994](#)), Lawrence Livermore National Labs OPAL opacity tables ([Iglesias & Rogers 1996](#)), and Los Alamos National Labs OPLIB opacity tables ([Colgan et al. 2016](#)).

The OPAL opacity tables in particular are very widely used by current generation stellar evolution programs (in addition to current generation stellar model and isochrone grids). However, they are no longer the most up-to-date elemental opacities or numerically precise. Moreover, the generation mechanism for these tables, a webform, is no longer reliably online.

Given its strong theoretical opacity dependence, it is reasonable to expect updated opacity tables to affect, the Jao Gap's mass range. Therefore, as part of this project we have transitioned DSEP from OPAL high temperature opacities to opacities based on measurements from Los Alamos national Labs T-1 group (OPLIB [Colgan et al. 2016](#)). This chapter in the thesis will detail the opacity transition, provide validation of the new opacity tables, and conduct an in-depth statistical comparison between the locations of Jao Gaps from populations modeled using both OPAL and OPLIB opacities.

Preliminary work shows populations modeled with OPLIB opacities have Jao Gaps at consistently lower masses / redder colors than those modeled using OPAL opacities (Figure 3 and Table 1). This is in line with expectations based on OPLIB opacities begin uniformly lower than OPAL opacities for temperature above  $10^6$  K (Figure 4) — with the lower opacities requiring commensurately lower core temperatures before radiation dominates energy transport.

## 2.2. Jao Gap Age-Dating - 1

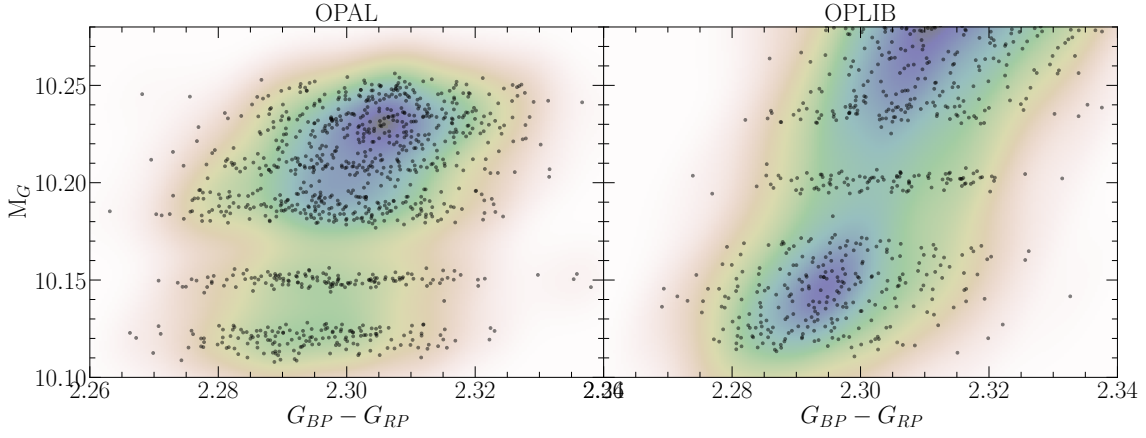


**Figure 3.** Synthetic CMDs derived from simple population synthesis code. (Left) CMD showing the Jao Gap for a GS98 composition stellar population generated from models evolved using OPAL opacity tables. (Right) CMD showing the Jao Gap for a GS98 stellar population generated from models evolved using the OPLIB opacity tables. Note how the OPLIB derived Jao Gap is slightly brighter than the OPAL Jao Gap.

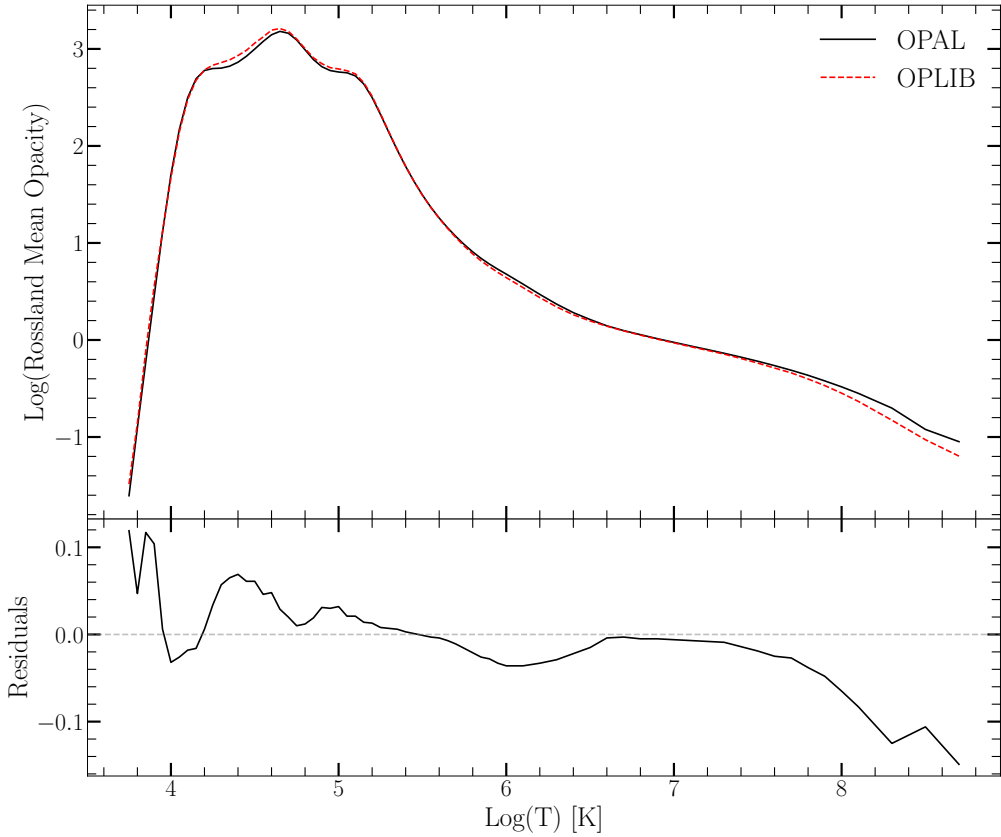


**Figure 4.** Rossland Mean Opacity from both OPAL (black solid) and OPLIB (red dashed). Note how above  $10^6$  K OPLIB opacities are uniformly smaller than those from OPAL.

| $Z =$ | $Z_{\odot}$    | 0.01            | 0.001           | 0.0001          |
|-------|----------------|-----------------|-----------------|-----------------|
| OPAL  | 0.3803 - 0.384 | 0.3583 - 0.3631 | 0.34 - 0.3448   | 0.362 - 0.3663  |
| OPLIB | 0.374 - 0.3767 | 0.3526 - 0.3567 | 0.3358 - 0.3406 | 0.3577 - 0.3621 |

**Table 1.** Mass ranges for the discontinuity in OPAL and OPLIB models. Masses are given in solar masses.

Following the integration of updated high temperature opacities detailed in §2.1, we will investigate using the observed color and magnitude range of the Jao Gap to age-date kinematically separated populations within the solar neighborhood.

While low-mass stars provide the majority of the fitting points for isochrones when estimating ages of clusters, due to the very slow variations in observables during main sequence evolution, it remains challenging to measure precise and accurate ages for low mass field stars (Soderblom 2010; Veyette & Muirhead 2018; Kiman et al. 2021). Moreover, the extremely high density of isochrones near the ZAMS, can result in uncertainties on isochrone age estimates for K and M dwarfs as high as 50 % (Lu et al. 2021). As a result of these high isochrone age uncertainties other methods of dating non-cluster populations have been developed, including age-calibrated rotation-activity relations (e.g. Kiman et al. 2021) and gyro-kinematic age-dating (e.g. Lu et al. 2021). In this chapter of the thesis we will present both a method of calibrating a Jao Gap location – age relation alongside a study of the mechanism driving a population’s Jao Gap location to evolve with age.

Both preliminary modeling and literature (e.g. Jao et al. 2018; Jao & Feiden 2020; Feiden et al. 2021; Mansfield & Kroupa 2021) demonstrate that the Jao Gap is expected to migrate along the main sequence as a population of stars age. Our modeling indicates that stellar populations younger than  $\sim 2$  Gyr do not show a gap. However, once the gap forms it will migrate towards bluer portions of the CMD with age.

For this proposal we do not perform any rigorous statistical testing of whether the differences in theoretical Jao Gap location could be discriminated between in observational data; instead, choosing to save that element of the research for thesis work proper. However, we do perform a qualitative

test of the visual distinguishability of the Jao Gap location in two CMDs with different sample sizes — 500 and 1000 stars (Figure 5).

**Move the equation so that it follow the reference in the text.**

$$\xi(m) = \xi_0 \left( \frac{m}{M_\odot} \right)^{-2.68 \pm 0.09} \quad (4)$$

We evolve models over an extremely finely sampled mass grid centered at the theoretical Jao Gap location for a GS98 solar composition population of stars. We then adopt the (Sollima 2019) IMF between 0.1 and 1  $M_\odot$  (Equation 4) to sample these evolved models. Model surface gravities, effective temperatures, and luminosities are transformed into Gaia magnitudes using bolometric correction tables provided by ESA<sup>1</sup> and color-code provided by Dotter.

Figure 5 shows the synthetic CMDs. Panels A and B show (1 Gyr) do not show any visible Jao Gap; whereas, Panels C, D, E, and F all do. Moreover, the location of the Gap visibly shifts to lower magnitudes from 3 Gyr to 6 Gyrs. Note that this shift is apparent in CMDs with both 1000s stars and those with 500 stars.

We use the Gaia Catalogue of Nearby Stars (NBS) to validate that the color range of the Jao Gap in separated populations could contain enough stars to distinguish these shifts. The NBS comprises a subset of all Gaia sources within 100 pc, it has been cleaned of spurious sources and is 92% complete for stars earlier than M9 with completeness dropping off for later spectral classes at the same distance (Gaia Collaboration et al. 2021). Querying the NBS yields 7654 sources within a tight color and magnitude band around the Jao Gap’s expected location (the same domain and range as in Figure 5).

**The actual stellar population model should include uncertainties in the photometry and parallaxes.**

Obviously, a simple visual identification is prone to confirmation bias and we are not considering variations in metallicity and binarity — both of which will obscure the Jao Gap — in this simple population synthetic model. However, given both the visual clear shift in our preliminary modeling

<sup>1</sup> [https://gea.esac.esa.int/archive/documentation/GDR2/Data\\_processing/chap\\_cu5pho/sec\\_cu5pho\\_calibr/ssec\\_cu5pho\\_calibr\\_extern.html](https://gea.esac.esa.int/archive/documentation/GDR2/Data_processing/chap_cu5pho/sec_cu5pho_calibr/ssec_cu5pho_calibr_extern.html)

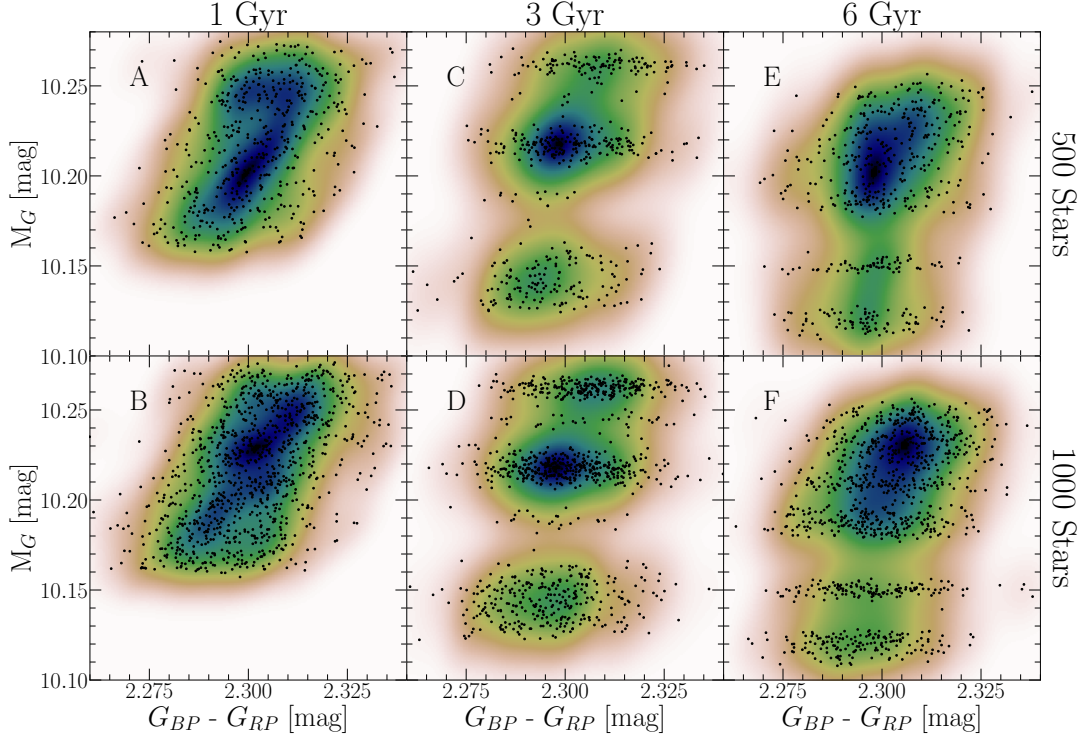


**Figure 5.** Populations synthesis results for a mass range surrounding the theoretical location of the Jao Gap at three population ages and with different sample sizes. The superimposed color map is derived from a Gaussian kernel-density-estimation run on the displayed points. This is included to better illustrate the gap location.

along with the volumn of empirical data Gaia provides, we believe that a more rigorous study is warrented.

Identifying the Jao Gap’s location is one part of this work, another part is to tie these shifts in gap location to established age proxies — that is we need to calibrate the Jao Gap’s age sensitivity. We propose to model a population of stars of various ages and metallicities sampled from [Holmberg et al. \(2009\)](#). Each of these stars will be assigned kinematics — again sampled from empirical distributions (Figure 6, [Lu et al. 2021](#)). We will then extract kinematically derived ages from this population and use these to segregate stars into rough age bins. We will measure if difference in Jao Gap locations are statistically distinguishable between these rough age bins, allowing us to extract the a priori ages.

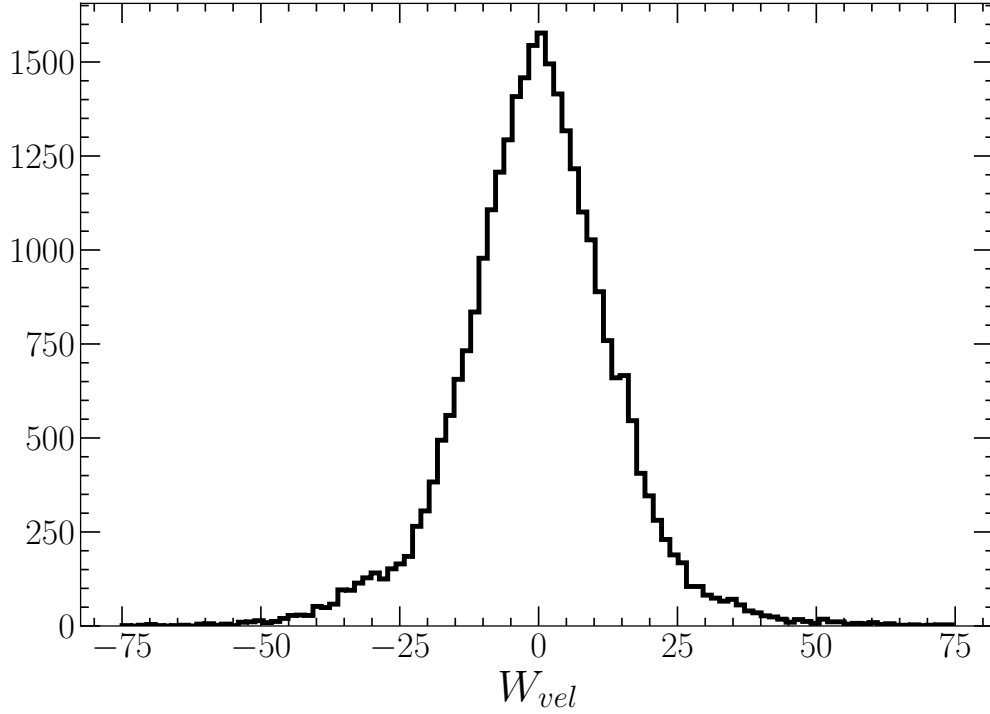


**Figure 6.** Distribution of vertical velocity displacement from [Lu et al. \(2021\)](#).

### 2.3. *Jao Gap Age-Dating - 2*

Where the project laid out in §2.2 will study the feasibility of using the Jao Gap to date stellar populations; this project will apply this technique to observational data. We will use Gaia photometry for the solar neighborhood to study whether the Jao Gap’s theoretical age-dependence is observable.

Our sample will be pulled from the NBS. It is known that the Jao Gap is observable in this sample (Figure 17 in [Gaia Collaboration et al. 2021](#)); however, we are less interested in if the gap shows up at all and instead interested in if subsets of the population show the gap in different locations. Using Gaia reported vertical velocity displacements and following methods from ([Lu et al. 2021](#)) we will slice the NBS into rough age groups (e.g.  $< 2$  Gyr,  $\geq 2$  and  $< 6$  Gyr, and  $\geq 6$  Gyr). Then, following binning methods laid out in [Jao et al. \(2018\)](#) we will measure the Jao Gap location for each group.

Both binarity and variations in metallicity will smear the Jao Gap. The Renormalised Unit Weight Error (RUWE) reported by Gaia, which tracks excess astrometric noise, can be used to filter for [Take a look at Penoyre et al. 2022 arXiv:2202.06963 for how to find binaries in NBS](#) wide binaries with mass ratios near 1 (e.g. [Deacon & Kraus 2020](#); [Kervella et al. 2022](#)). Further, we can model populations assuming an M Dwarf binary fraction [[Jen Winters Paper on local Binarity](#)] to place bounds on gap and gap shift detectability. Similarly we will adopt a metallicity function for the solar neighborhood (though this is approximately constant) ([Holmberg et al. 2009](#)) when modeling the gap to place bounds on it and its shift detectability.

#### 2.4. *NGC 2808*

Whereas, people have have often tried to categorized objects as GCs by making cuts along half-light radius, density, and surface brightness profile, in fact many objects which are generally thought of as GCs don't cleanly fit into these cuts. Consequently, [Carretta et al. \(2010\)](#) proposed a definition of GC based on observed chemical inhomogeneities in their stellar populations. The modern understanding of GCs then is not simply one of a dense cluster of stars which may have chemical inhomogeneities and multiple populations; rather, it is one where those chemical inhomogeneities and multiple populations themselves are the defining element of a GC.

All globular clusters older than 2 Gyr studied in detail show populations enriched in He, N, and Na while also being deplete in O and C ([Piotto et al. 2015](#); [Bastian & Lardo 2018](#)). These light element abundance patterns also are not strongly correlated with variations in heavy element abundances. One consequence of this fact is the spectroscopically uniform Fe abundances mentioned in §1.1. Further, high-resolution spectral studies reveal anti-correlations between N-C abundances, Na-O abundances, and potentially Al-Mg ([Snedden et al. 1992](#); [Gratton et al. 2012](#)). Typical stellar fusion reactions can deplete core oxygen; however, the observed abundances of Na, Al, and Mg cannot be explained by the likes of the CNO cycle ([Prantzos et al. 2007](#)).

Formation channels for these multiple populations remain a point of debate among astronomers. Most proposed formation channels consist of some older, more massive, population of stars polluting the pristine cluter media before a second population forms, now enriched in heavier elements which

they themselves could not have generated (for a detailed review see [Gratton et al. 2012](#)). The four primary candidates for these polluters are asymptotic giant branch stars (AGBs, [Ventura et al. 2001](#); [D’Ercole et al. 2010](#)), fast rotating massive stars (FRMSs, [Decressin et al. 2007](#)), super massive stars (SMSs, [Denissenkov & Hartwick 2014](#)), and massive interacting binaries (MIBs, [de Mink et al. 2009](#); [Bastian & Lardo 2018](#)).

Hot hydrogen burning (proton capture), material transport to the surface, and material ejection into the intra-cluster media are features of each of these models and consequently they can all be made to *qualitatively* agree with the observed elemental abundances. However, none of the standard models can currently account for all specific abundances ([Gratton et al. 2012](#)). AGB and FRMS models are the most promising; however, both models have difficulty reproducing severe O depletion ([Ventura & D’Antona 2009](#); [Decressin et al. 2007](#)). Moreover, AGB and FRMS models require significant mass loss ( $\sim 90\%$ ) between cluster formation and the current epoch — implying that a significant fraction of halo stars formed in GCs ([Renzini 2008](#); [D’Ercole et al. 2008](#); [Bastian & Lardo 2015](#)).

In addition to the light-element anti-correlations observed it is also known that younger populations are significantly enhanced in Helium ([Piotto et al. 2007, 2015](#); [Latour et al. 2019](#)). Depending on the cluster, Helium mass fractions as high as  $Y = 0.4$  have been inferred (e.g [Milone et al. 2015](#)). However, due to the relatively high and tight temperature range of partial ionization for He it cannot be observed in globular clusters; consequently, the evidence for enhanced He in GCs originates from comparison of theoretical stellar isochrones to the observed color-magnitude-diagrams of globular clusters. Therefore, a careful handling of chemistry is essential when modeling with the aim of discriminating between MPs; yet, only a very limited number of GCs have yet been studied with chemically self-consistent (structure and atmosphere) isochrones (e.g. [Dotter et al. 2015](#), NGC 6752).

This thesis will contain chapters where we expand the number of clusters which have been self-consistently modeled. In this chapter we will focus on chemically self-consistent modeling of the two extreme population of NGC 2808 identified by ([Milone et al. 2015](#)), A and E.



One key element of NGC 2808 modeling is the incorporation of new atmospheric models, generated from the MARCS grid of model atmospheres (Plez 2008), which match interior elemental abundances. MARCS provides one-dimensional, hydrostatic, plane-parallel and spherical LTE atmospheric models (Gustafsson et al. 2008). Members of our collaboration have generated atmospheric models for populations A and E. Integration of these new model atmospheres into DSEP is ongoing.

#### 2.4.1. *Population Opacities*

For similar reasons as discussed in §2.1 we conduct this research with OPLIB high-temperature opacity tables as opposed to OPAL tables. We will also generate low temperature opacity tables using the MARCS [CODE]. Moreover, we confirm that the atmosphere and structure meet in an optically thick region of the star by shifting the atmospheric fitting point from an optical depth of  $\tau = 2/3$  (used by DSEP currently for PHOENIX model atmospheres) to some higher  $\tau$ . We will experiment to identify the best optical depth to fit at..

These population have been studied in depth by Feiden and their chemical compositions were determined in Milone et al. (2015) (see Table 2 in that paper). While we cannot yet evolve DSEP models with these new boundary conditions, we can make a first pass investigation of the affect of OPLIB opacities (Figure 7). Note how the models generated using OPLIB opacity tables have a systematically lower luminosity. This discrepancy is consistent with the overall lower opacities of the OPLIB tables.

#### 2.4.2. *Additional Consistency*

The isochrones generally used to infer the degree of helium enhancements assume that convection operates in the same manner in metal-poor stars as it does in the Sun. However, observations from *Kepler* of metal-poor red giants (Bonaca et al. 2012; Tayar et al. 2017), in concert with interferometric radius determination of the metal-poor sub-giant HD 140283 (Creevey et al. 2015), have shown that the efficiency of convection changes with iron content. As the final portion of our work to more carefully handle a stars chemistry, we will modify DSEP to capture this variation in convective efficiency.

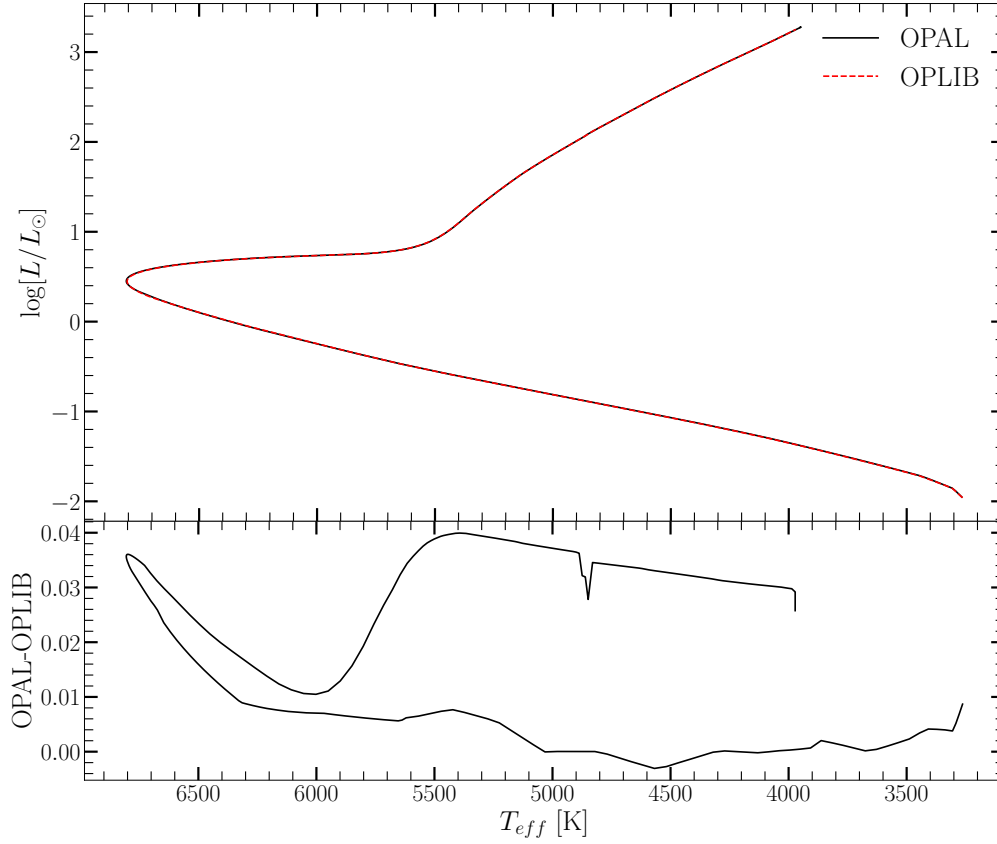


**Figure 7.** 10 Gyr &  $Y=0.33$  isochrones for models generated with OPAL and OPLIB opacities tables (top). Residuals between isochrones (bottom).

### 2.5. *47 Tuc* & *NGC 6752*

In addition to NGC 2808, collaborators will generate MARCS atmospheric boundary conditions for multiple populations within the clusters NGC 6752 and 47 Tuc. Using these surface boundary conditions along with new opacity tables we query from OPLIB, we will conduct the same, self-consistent, modeling for these clusters as we do for NGC 2808.

NGC 6752 has been self-consistently modeled in past. [Dotter et al. \(2015\)](#) perform self-consistent chemical modeling of this cluster using both ATLAS and PHOENIX atmospheric boundary conditions computed from abundance of the photometrically identified populations A and C reported by [Milone et al. \(2013\)](#). [Dotter et al.](#) additionally make use of OPAL high temperature opacity tables and PHOENIX low temperature opacity tables.

[Dotter et al.](#) find slight difference between best fit isochrone to NGC 6752 populations A and E for both blue and UV synthetic CMDs, with ATLAS atmospheres performing slightly better. Moreover, they find that the inferred helium abundance is sensitive to atmospheric boundary conditions, with ATLAS models showing stronger helium sensitivity than PHOENIX models.

We will replicate portions of the work [Dotter et al.](#) conduct on NGC 6752 and extend this work to 47 Tuc. Of particular interest is MARCS historical focus on earlier spectral class stars and commensurately on bluer portions of the model atmosphere when compared to PHOENIX [\[CITE\]](#), and how this will affect inferred elemental abundances. [Dotter et al.](#) find the primary difference between ATLAS and PHOENIX models originating from UV difference in their spectra.

### 3. THESIS TIMELINE

We propose a thesis in five parts. Hereafter, the papers which will form the chapters of the thesis will be referred to P1, P2, P3, P4, and P5. These are enumerated in chronological order of submission.

The first paper, P1, detailing work already done to update DSEP to OPLIB opacity tables and the effects those new opacity tables have on the Jao Gap location will be submitted in the summer of 2022. The primary outstanding work for P1 is to run population synthesis models as, observationally, the Jao Gap is observed in populations of stars.

P2 covering self consistent modeling of NGC 2808, will be submitted sometime between the start of the fall 2022 term and the spring 2023 term. Per Section [2.4](#) much of the background work for this paper has been completed and we are currently ramping up modeling efforts now that we have atmospheric models in hand. P4, consisting of modeling of both 47 Tuc and NGC 6752 will follow directly from this work. Given P4's similarity to P2 we anticipate it will only take three terms to submit, with an expected submission term of summer 2023.

P3 will be submitted in the spring of 2023. This paper will focus on modeling populations of low mass stars in the local solar neighborhood in order to determine if the location of the Jao Gap in the CMD may be used to date these populations. Work on this paper has not yet begun. Finally,

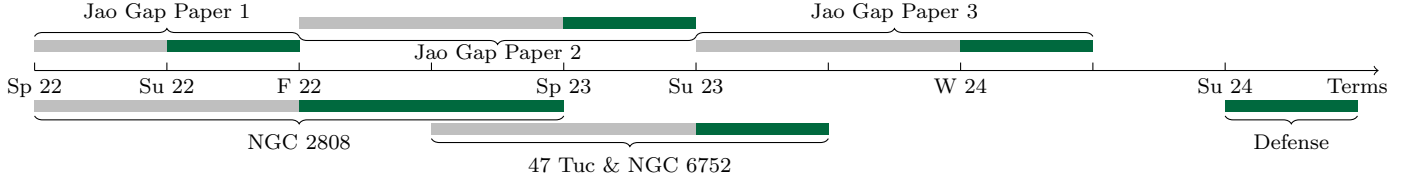


**Figure 8.** Proposed timeline for thesis work. Terms where a paper is expected to be submitted are marked with green, terms where work on a project is intended to take place are marked in grey.

P5 will follow up on the theoretical work from the P3; gathering archival photometric data from low-mass stars in the local solar neighborhood and comparing Jao Gap derived ages to ages derived from the age-velocity-dispersion relation.

These five papers, in addition to an introductory chapter, will comprise a thesis to be defended sometime in the Summer 2024 term.

## REFERENCES

- Anderson, J., Piotto, G., King, I., Bedin, L., & Guhathakurta, P. 2009, *The Astrophysical Journal Letters*, 697, L58
- Baraffe, I., & Chabrier, G. 2018, *A&A*, 619, A177, doi: [10.1051/0004-6361/201834062](https://doi.org/10.1051/0004-6361/201834062)
- Bastian, N., & Lardo, C. 2015, *MNRAS*, 453, 357, doi: [10.1093/mnras/stv1661](https://doi.org/10.1093/mnras/stv1661)
- Bastian, N., & Lardo, C. 2018, *Annual Review of Astronomy and Astrophysics*, 56, 83
- Bjork, S. R., & Chaboyer, B. 2006, *ApJ*, 641, 1102, doi: [10.1086/500505](https://doi.org/10.1086/500505)
- Bonaca, A., Tanner, J. D., Basu, S., et al. 2012, *The Astrophysical Journal Letters*, 755, L12, doi: [10.1088/2041-8205/755/1/L12](https://doi.org/10.1088/2041-8205/755/1/L12)
- Carretta, E., Bragaglia, A., Gratton, R. G., et al. 2010, *Astronomy & Astrophysics*, 516, A55
- Chaboyer, B., Fenton, W. H., Nelan, J. E., Patnaude, D. J., & Simon, F. E. 2001, *ApJ*, 562, 521, doi: [10.1086/323872](https://doi.org/10.1086/323872)
- Chabrier, G., & Baraffe, I. 1997, *A&A*, 327, 1039. <https://arxiv.org/abs/astro-ph/9704118>
- Colgan, J., Kilcrease, D. P., Magee, N. H., et al. 2016, in *APS Meeting Abstracts*, Vol. 2016, APS Division of Atomic, Molecular and Optical Physics Meeting Abstracts, D1.008
- Collaboration, P., et al. 2016, XIII. Cosmological parameters
- Cowling, T. G. 1966, *QJRAS*, 7, 121

- Creevey, O., Thévenin, F., Berio, P., et al. 2015, *Astronomy & Astrophysics*, 575, A26
- de Mink, S. E., Pols, O. R., Langer, N., & Izzard, R. G. 2009, *A&A*, 507, L1, doi: [10.1051/0004-6361/200913205](https://doi.org/10.1051/0004-6361/200913205)
- Deacon, N. R., & Kraus, A. L. 2020, *Monthly Notices of the Royal Astronomical Society*, 496, 5176, doi: [10.1093/mnras/staa1877](https://doi.org/10.1093/mnras/staa1877)
- Decressin, T., Meynet, G., Charbonnel, C., Prantzos, N., & Ekström, S. 2007, *A&A*, 464, 1029, doi: [10.1051/0004-6361:20066013](https://doi.org/10.1051/0004-6361:20066013)
- Denissenkov, P. A., & Hartwick, F. D. A. 2014, *MNRAS*, 437, L21, doi: [10.1093/mnras/slt133](https://doi.org/10.1093/mnras/slt133)
- D’Ercole, A., D’Antona, F., Ventura, P., Vesperini, E., & McMillan, S. L. W. 2010, *MNRAS*, 407, 854, doi: [10.1111/j.1365-2966.2010.16996.x](https://doi.org/10.1111/j.1365-2966.2010.16996.x)
- D’Ercole, A., Vesperini, E., D’Antona, F., McMillan, S. L. W., & Recchi, S. 2008, *MNRAS*, 391, 825, doi: [10.1111/j.1365-2966.2008.13915.x](https://doi.org/10.1111/j.1365-2966.2008.13915.x)
- Dotter, A., Chaboyer, B., Jevremović, D., et al. 2008, *The Astrophysical Journal Supplement Series*, 178, 89
- Dotter, A., Ferguson, J. W., Conroy, C., et al. 2015, *MNRAS*, 446, 1641, doi: [10.1093/mnras/stu2170](https://doi.org/10.1093/mnras/stu2170)
- D’Antona, F., Bellazzini, M., Caloi, V., et al. 2005, *The Astrophysical Journal*, 631, 868
- Emden, R. 1907, *Gaskugeln*
- Feiden, G. A., Skidmore, K., & Jao, W.-C. 2021, *ApJ*, 907, 53, doi: [10.3847/1538-4357/abcc03](https://doi.org/10.3847/1538-4357/abcc03)
- Gaia Collaboration, Smart, R. L., Sarro, L. M., et al. 2021, *A&A*, 649, A6, doi: [10.1051/0004-6361/202039498](https://doi.org/10.1051/0004-6361/202039498)
- Gratton, R., Sneden, C., & Carretta, E. 2004, *ARA&A*, 42, 385, doi: [10.1146/annurev.astro.42.053102.133945](https://doi.org/10.1146/annurev.astro.42.053102.133945)
- Gratton, R. G., Carretta, E., & Bragaglia, A. 2012, *Astronomy and Astrophysics Reviews*, 20, 50, doi: [10.1007/s00159-012-0050-3](https://doi.org/10.1007/s00159-012-0050-3)
- Gratton, R. G., Bonifacio, P., Bragaglia, A., et al. 2001, *A&A*, 369, 87, doi: [10.1051/0004-6361:20010144](https://doi.org/10.1051/0004-6361:20010144)
- Gustafsson, B., Edvardsson, B., Eriksson, K., et al. 2008, *A&A*, 486, 951, doi: [10.1051/0004-6361:200809724](https://doi.org/10.1051/0004-6361:200809724)
- Herschel, W. 1814, *Philosophical Transactions of the Royal Society of London*, 248
- Holmberg, J., Nordström, B., & Andersen, J. 2009, *A&A*, 501, 941, doi: [10.1051/0004-6361/200811191](https://doi.org/10.1051/0004-6361/200811191)
- Iglesias, C. A., & Rogers, F. J. 1996, *ApJ*, 464, 943, doi: [10.1086/177381](https://doi.org/10.1086/177381)
- Jao, W.-C., & Feiden, G. A. 2020, *AJ*, 160, 102, doi: [10.3847/1538-3881/aba192](https://doi.org/10.3847/1538-3881/aba192)
- Jao, W.-C., Henry, T. J., Gies, D. R., & Hambly, N. C. 2018, *ApJL*, 861, L11, doi: [10.3847/2041-8213/aacdf6](https://doi.org/10.3847/2041-8213/aacdf6)
- Kervella, P., Arenou, F., & Thévenin, F. 2022, *A&A*, 657, A7, doi: [10.1051/0004-6361/202142146](https://doi.org/10.1051/0004-6361/202142146)

- Kiman, R., Faherty, J. K., Cruz, K. L., et al. 2021, *AJ*, 161, 277, doi: [10.3847/1538-3881/abf561](https://doi.org/10.3847/1538-3881/abf561)
- Kovetz, A., Yaron, O., & Prialnik, D. 2009, *MNRAS*, 395, 1857, doi: [10.1111/j.1365-2966.2009.14670.x](https://doi.org/10.1111/j.1365-2966.2009.14670.x)
- Latour, M., Husser, T. O., Giesers, B., et al. 2019, *A&A*, 631, A14, doi: [10.1051/0004-6361/201936242](https://doi.org/10.1051/0004-6361/201936242)
- Lu, Y. L., Angus, R., Curtis, J. L., David, T. J., & Kiman, R. 2021, *AJ*, 161, 189, doi: [10.3847/1538-3881/abe4d6](https://doi.org/10.3847/1538-3881/abe4d6)
- Mansfield, S., & Kroupa, P. 2021, *A&A*, 650, A184, doi: [10.1051/0004-6361/202140536](https://doi.org/10.1051/0004-6361/202140536)
- Milone, A., Marino, A., Piotto, G., et al. 2012, *The Astrophysical Journal*, 745, 27
- Milone, A. P., Marino, A. F., Piotto, G., et al. 2013, *ApJ*, 767, 120, doi: [10.1088/0004-637X/767/2/120](https://doi.org/10.1088/0004-637X/767/2/120)
- . 2015, *ApJ*, 808, 51, doi: [10.1088/0004-637X/808/1/51](https://doi.org/10.1088/0004-637X/808/1/51)
- Norris, J. 1987, *The Astrophysical Journal*, 313, L65
- Osborn, W. 1971, *The Observatory*, 91, 223
- Paxton, B., Bildsten, L., Dotter, A., et al. 2011, *The Astrophysical Journal Supplement Series*, 192, 3, doi: [10.1088/0067-0049/192/1/3](https://doi.org/10.1088/0067-0049/192/1/3)
- Piotto, G., Bedin, L. R., Anderson, J., et al. 2007, *The Astrophysical Journal Letters*, 661, L53, doi: [10.1086/518503](https://doi.org/10.1086/518503)
- Piotto, G., Milone, A. P., Bedin, L. R., et al. 2015, *AJ*, 149, 91, doi: [10.1088/0004-6256/149/3/91](https://doi.org/10.1088/0004-6256/149/3/91)
- Plez, B. 2008, *Physica Scripta Volume T*, 133, 014003, doi: [10.1088/0031-8949/2008/T133/014003](https://doi.org/10.1088/0031-8949/2008/T133/014003)
- Prantzos, N., Charbonnel, C., & Iliadis, C. 2007, *A&A*, 470, 179, doi: [10.1051/0004-6361:20077205](https://doi.org/10.1051/0004-6361:20077205)
- Renzini, A. 2008, *Monthly Notices of the Royal Astronomical Society*, 391, 354, doi: [10.1111/j.1365-2966.2008.13892.x](https://doi.org/10.1111/j.1365-2966.2008.13892.x)
- Rodríguez-López, C. 2019, *Frontiers in Astronomy and Space Sciences*, 6, 76, doi: [10.3389/fspas.2019.00076](https://doi.org/10.3389/fspas.2019.00076)
- Sandage, A. R. 1953, *AJ*, 58, 61, doi: [10.1086/106822](https://doi.org/10.1086/106822)
- Seaton, M. J., Yan, Y., Mihalas, D., & Pradhan, A. K. 1994, *MNRAS*, 266, 805, doi: [10.1093/mnras/266.4.805](https://doi.org/10.1093/mnras/266.4.805)
- Snedden, C., Kraft, R. P., Prosser, C. F., & Langer, G. 1992, *The Astronomical Journal*, 104, 2121
- Soderblom, D. R. 2010, *ARA&A*, 48, 581, doi: [10.1146/annurev-astro-081309-130806](https://doi.org/10.1146/annurev-astro-081309-130806)
- Sollima, A. 2019, *Monthly Notices of the Royal Astronomical Society*, 489, 2377, doi: [10.1093/mnras/stz2093](https://doi.org/10.1093/mnras/stz2093)
- Stetson, P. B., & Harris, W. E. 1988, *The Astronomical Journal*, 96, 909, doi: [10.1086/114856](https://doi.org/10.1086/114856)

- Tayar, J., Somers, G., Pinsonneault, M. H., et al. 2017, *The Astrophysical Journal*, 840, 17
- van Saders, J. L., & Pinsonneault, M. H. 2012, *ApJ*, 751, 98, doi: [10.1088/0004-637X/751/2/98](https://doi.org/10.1088/0004-637X/751/2/98)
- Ventura, P., & D’Antona, F. 2009, *A&A*, 499, 835, doi: [10.1051/0004-6361/200811139](https://doi.org/10.1051/0004-6361/200811139)
- Ventura, P., D’Antona, F., Mazzitelli, I., & Gratton, R. 2001, *ApJL*, 550, L65, doi: [10.1086/319496](https://doi.org/10.1086/319496)
- Veyette, M. J., & Muirhead, P. S. 2018, *ApJ*, 863, 166, doi: [10.3847/1538-4357/aad40e](https://doi.org/10.3847/1538-4357/aad40e)
- Vinyoles, N., Serenelli, A. M., Villante, F. L., et al. 2017, *The Astrophysical Journal*, 835, 202